Science of the Total Environment 814 (2022) 152732

Contents lists available at ScienceDirect

Science of the Total Environment

journal homepage: www.elsevier.com/locate/scitotenv

Single PFAS and PFAS mixtures affect nuclear receptor- and oxidative stress-related pathways in precision-cut liver slices of Atlantic cod (*Gadus morhua*)

Karina Dale [a], Fekadu Yadetie [a], Torill Horvli [a], Xiaokang Zhang [b], Håvard Guldbrandsen Frøysa [c], Odd André Karlsen [a], Anders Goksøyr [a,*]

[a] Department of Biological Sciences, University of Bergen, Thormøhlensgate 53B, 5006 Bergen, Norway
[b] Department of Molecular Oncology, Institute for Cancer Research, Oslo University Hospital-Radiumhospitalet, Vestenghaugen 8, 0379 Oslo, Norway
[c] Institute of Marine Research, Nordnesgaten 50, NO-5005 Bergen, Norway

HIGHLIGHTS

- Marine organisms are exposed to complex mixtures of environmental contaminants.
- Single and mixture toxicity of *per*-and-polyfluoroalkyl substances (PFAS) was studied.
- Transcriptomic responses of cod precision-cut liver slices (PCLS) were assessed.
- PFAS affected nuclear receptor- and stress-related pathways in cod PCLS.
- Interactive effects of PFAS can occur in mixture exposures.

GRAPHICAL ABSTRACT

A graphical abstract is mandatory for this journal. It should summarize the contents of the article in a concise, pictorial form designed to capture the attention of a wide readership online. Authors must provide images that clearly represent the work described in the article. Graphical abstracts should be submitted as a separate file in the online submission system. Image size: please provide an image with a minimum of 531 × 1328 pixels (h × w) or proportionally more. The image should be readable at a size of 5 × 13 cm using a regular screen resolution of 96 dpi. Preferred file types: TIFF, EPS, PDF or MS Office files. You can view Example Graphical Abstracts on our information site.

Authors can make use of Elsevier's Illustration Services to ensure the best presentation of their images also in accordance with all technical requirements.

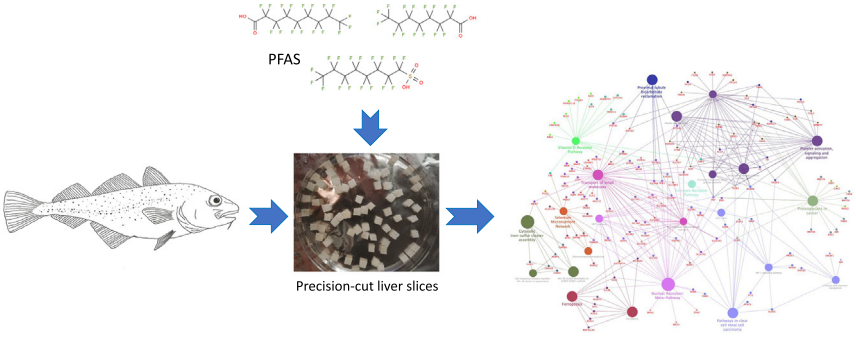

Abbreviations: Acyl coenzyme-A oxidase 1, Acox1; Acyl coenzyme-A synthetase long-chain family member 4, Acsl4; Antioxidant response element, Are; Aryl hydrocarbon receptor, Ahr; ATP binding cassette, Abc; ATP citrate lyase, Acly; Catalase, Cat; Cytochrome P450, Cyp; Dimethyl sulfoxide, DMSO; False discovery rate, FDR; Farnesoid X receptor, Fxr; Fatty acid synthase, Fasn; Glutathione cysteine ligase catalytic unit, Gclc; Glutathione cysteine ligase modifier unit, Gclm; Glucose-6-phosphate dehydrogenase, G6pd; Glutathione-S-transferase, Gst; Mechanistic target of rapamycin complex 1, mTORC1; Mode of action, MoA; Nuclear factor erythroid 2-related factor 2, Nrf2; Organic anion transporting polypeptides, Oatp; Per- and polyfluoroalkyl substances, PFAS; Perfluoroalkyl carboxylates, PFCA; Perfluoroalkane sulfonates, PFSA; Perfluorononanoate, PFNA; Perfluorooctane sulfonate, PFOS; Perfluorooctanoate, PFOA; Peroxiredoxin, Prdx; Peroxisome proliferator, PP; Peroxisome proliferator-activated receptor, Ppar; Persistent organic pollutant, POP; Polyunsaturated fatty-acid containing phospholipids, PUFA-PL; Precision-cut liver slices, PCLS; Retinoid X receptor, Rxr; Solute carrier, Slc; Superoxide dismutase, Sod; Thioredoxin reductase, Txnrd; Transmembrane protein, Tmem.

* Corresponding author at: Department of Biological Sciences, University of Bergen, Thormøhlensgate 53B, N-5006 Bergen, Norway.
E-mail addresses: karina.dale@stim.no (K. Dale), Fekadu.Yadetie@uib.no (F. Yadetie), Xiaokang.Zhang@rr-research.no (X. Zhang), haavard.guldbrandsen.froeysa@hi.no (H.G. Frøysa), Odd.Karlsen@uib.no (O.A. Karlsen), anders.goksoyr@uib.no (A. Goksøyr).

http://dx.doi.org/10.1016/j.scitotenv.2021.152732

ARTICLE INFO

Article history:
Received 4 November 2021
Received in revised form 9 December 2021
Accepted 23 December 2021
Available online 31 December 2021

Editor: Adrian Covaci

Keywords:
Perfluoroalkyl acids (PFAA)
PFOS
Mixture toxicity
Cholesterol
Ferroptosis
Fish

ABSTRACT

The aim of the present study was to investigate effects of *per*- and polyfluoroalkyl substances (PFAS), both single compounds and a mixture of these, using precision-cut liver slices (PCLS) from Atlantic cod (*Gadus morhua*). PCLS were exposed for 48 h to perfluorooctane sulfonate (PFOS), perfluorooctanoate (PFOA) and perfluorononanoate (PFNA) (10, 50 and 100 μM), and three mixtures of these at equimolar concentrations (10, 50 and 100 μM). Transcriptomic responses were assessed using RNA sequencing. Among exposures to single PFAS, PFOS produced the highest number of differentially expressed genes (DEGs) compared to PFOA and PFNA (86, 25 and 31 DEGs, respectively). Exposure to the PFAS mixtures resulted in a markedly higher number of DEGs (841). Clustering analysis revealed that the expression pattern of the PFAS mixtures were more similar to PFOS compared to PFOA and PFNA, suggesting that effects induced by the PFAS mixtures may largely be attributed to PFOS. Pathway analysis showed significant enrichment of pathways related to oxidative stress, cholesterol metabolism and nuclear receptors in PFOS-exposed PCLS. Fewer pathways were significantly enriched following PFOA and PFNA exposure alone. Significantly enriched pathways following mixture exposure included lipid biosynthesis, cancer-related pathways, nuclear receptor pathways and oxidative stress-related pathways such as ferroptosis. The expression of most of the genes within these pathways was increased following PFAS exposure. Analysis of non-additive effects in the 100 μM PFAS mixture highlighted genes involved in the antioxidant response and membrane transport, among others, and the majority of these genes had synergistic expression patterns in the mixture. Nevertheless, 90% of the DEGs following mixture exposure showed additive expression patterns, suggesting additivity to be the major mixture effect. In summary, PFAS exposure promoted effects on cellular processes involved in oxidative stress, nuclear receptor pathways and sterol metabolism in cod PCLS, with the strongest effects observed following PFAS mixture exposure.

1. Introduction

Marine ecosystems are sinks for environmental contaminants originating from both land-based run-off and offshore activities (Windom, 1992). Organisms are thus exposed to complex mixtures of anthropogenic contaminants. Despite this, risk assessment of contaminants does not usually reflect such intricate exposure scenarios, as they often rely heavily on single compound toxicity studies (Bopp et al., 2019). Mixture effects have received increased attention in the past years, *e.g.*, through various EU research activities (Bopp et al., 2018), and further work is needed to understand the combined effects of contaminants on biological systems. This is of crucial importance as combining chemicals might produce effects that are stronger (synergism) or weaker (antagonism) compared to additive effects (Celander, 2011), the latter being the standard procedure of assessing toxicity of contaminant mixtures (Cedergreen, 2014).

Per- and polyfluoroalkyl substances (PFAS) are synthetic, organic compounds whose chemical and thermal properties have led to extensive use in consumer products, including fire-fighting foams, paint, and as waterproof and stain-resistant material. However, these properties are also the reason why these chemicals are persistent and potent environmental contaminants (Ahrens, 2011). The bioaccumulation potential of PFAS in biota is related to their high affinity to fatty acid binding proteins and serum albumin (Ahrens and Bundschuh, 2014). Among PFAS, there are two important subclasses of the fully fluorinated perfluoroalkyl acids (PFAAs): the perfluoroalkane sulfonates (PFSAs) and perfluoroalkyl carboxylates (PFCAs). These subclasses include some well-studied compounds such as perfluorooctane sulfonate (PFOS), which is known to predominate among PFAS in biota (Sturm and Ahrens, 2010), perfluorooctanoate (PFOA), and perfluorononanoate (PFNA) (Buck et al., 2011). PFOS and its precursor and salts were added to Annex B of the Stockholm Convention in 2009, and PFOA with its related compounds have been reviewed by the POP Review Committee since 2015. In 2020, five European countries, including Norway, proposed a total ban of production and use of all PFAS (Norwegian Environment Agency, 2020).

Recently, adverse effects of exposure to PFAAs in fish and other aquatic organisms were summarized, highlighting effects such as reproductive and developmental toxicity, metabolic disruption, and oxidative stress (Lee et al., 2020). Additionally, some studies have investigated biological responses following exposure to PFAS mixtures. Combined PFOS and PFOA exposure were shown to promote antagonistic effects in the cyanobacterium *Anabaena* CPB4337 (Rodea-Palomares et al., 2015), compared to synergistic effects observed in the crustacean *Daphnia magna* (H.-B. Yang et al., 2019). Contradicting results have also been observed in studies involving more complex PFAS mixtures. A mixture of nine PFAS has been shown to reduce the potencies of individual PFAS in zebrafish (*Danio rerio*) embryos (Menger et al., 2020). In contrast, a large variety of binary, ternary and multi-component PFAS mixtures displayed mostly synergistic effects on cell viability of human HepG2 cells (Ojo et al., 2020). These findings underline the complexity of investigating and understanding biological effects of PFAS mixtures, an issue which needs to be further addressed.

Atlantic cod (*Gadus morhua*) is an important commercial teleost species in the North Atlantic, and is also utilized in monitoring programs in northern Europe (Hylland et al., 2008; Sundt et al., 2012). Facilitated by the availability of the sequenced and annotated cod genome (Star et al., 2011; Tørresen et al., 2017), Atlantic cod has become a popular model organism in environmental toxicology, including studies using omics-based approaches (Dale et al., 2020; Khan et al., 2021; Yadetie et al., 2018). Compared to many other fish species, the cod liver is particularly lipid-rich, with hepatocytes containing large lipid droplets. As many pollutants are lipid-soluble, they tend to accumulate in cod liver, making the liver a well-suited organ for investigating contaminant-induced toxicity. However, the high lipid content makes it difficult to isolate and use primary hepatocytes (Søfteland et al., 2010). An alternative way of using cod liver in toxicological studies is the application of precision-cut liver slices (PCLS). The PCLS technique is an *ex vivo* approach for studying hepatic responses in a manner that maintains the three-dimensional tissue structure of cell distribution, providing closer prediction of *in vivo* toxicity compared to *in vitro* techniques, including cell cultures (Eide et al., 2014). It is also shown that gene expression patterns in liver slices are more similar to expression patterns *in vivo*, compared to those in primary hepatocyte cultures (Boess et al., 2003). Furthermore, the method is efficient as several contaminants can be tested simultaneously with limited number of subjects, thereby reducing the number of fish needed in accordance with the 3R principles. Finally, the combination of PCLS and omics approaches facilitates mechanistic studies and the discovery of new biomarkers by generating high-throughput data for a large number of exposure scenarios (Brockmeier et al., 2017; Yadetie et al., 2018, 2021).

Limited knowledge exists on biological effects of PFAS exposure in fish, especially with regards to PFAS mixtures. Recently, we have shown that a similar PFAS mixture can affect lipid metabolism in Atlantic cod liver after *in vivo* exposure (Dale et al., 2020). In the present study, the PCLS technique was applied with Atlantic cod and combined with toxicogenomics (RNA-seq) to study effects of PFOS, PFOA and PFNA, both separately and in ternary equimolar mixtures. In this way, we aimed to obtain increased understanding of molecular and cellular effects following PFAS exposure in fish.

2. Methods

2.1. Fish husbandry

Juvenile Atlantic cod (*Gadus morhua*) were provided from Havbruksstasjonen in Tromsø AS (Tromsø, Norway), and maintained

at the Industrial and Aquatic Research Laboratory (ILAB, Bergen, Norway). The cod were kept in 500 L tanks with natural seawater at 9 °C with a 12:12 h light cycle regime and fed *ad libitum* with a commercial marine diet (Amber Neptune, Skretting, Stavanger, Norway). For liver slicing, cod weighing 690 ± 210 g (n = 8, six males and two females) were killed with a blow to the head and the liver excised and kept in cold PCLS buffer (NaCl 122 mM, KCl 4.8 mM, $MgSO_4$ 1.2 mM, Na_2HPO_4 11 mM and $NaHCO_3$ 3.7 mM, pH 8.4). Sex was determined by inspecting the gonads during dissection of the liver. No chemical exposure was performed on live fish and the fish were handled and euthanized according to national regulations and animal care standards by the Norwegian Food Safety Authority.

2.2. Precision-cut liver slices (PCLS) and exposure set-up

PCLS from four individual cod per exposure were prepared and exposed as described in Yadetie et al. (2018), with the following modifications: the liver was cut into 2 cm thick blocks using a scalpel, 250 μm slices were cut using a Leica VT1200 S vibrating blade vibratome (Leica, Wetzlar, Germany), and further divided into 4 × 4 mm pieces using a razor blade. The liver slices were kept in growth medium (Leibowitz-15 medium from Life Technologies™ Gibco®, Paisley, UK) supplemented with 10% charcoal-stripped and heat-inactivated fetal bovine serum and 1% penicillin-streptomycin–amphotericin (10,000 U/mL potassium penicillin, 10,000 μg/mL streptomycin and 25 μg/mL amphotericin B from Sigma Aldrich/Merck) at 4 °C. The liver slices were transferred to a 12-well plate (four slices per well) and pre-incubated in growth medium at 10 °C for 2 h prior to exposure. In addition, slices (one per well) were incubated in a separate 12-well plate for viability assays. A paired sample design (Salkind, 2010) was used where slices from each fish were used in all treatment groups, providing both control and exposed conditions (individual fish are biological replicates).

PCLS were exposed to PFAS by replacing the growth medium with fresh medium (1 mL) containing DMSO vehicle control (0.1%) or selected chemicals at different concentrations (Table 1 and Table S1) dissolved in DMSO. The exposures were divided into two separate experiments (single PFAS separated from the mixtures, n = 4 fish per experiment) with separate DMSO control for each experiment (denoted DMSO_s and DMSO_m where relevant). In experiment I (single compound treatments), liver slices from each of four (one female and three male) fish (biological replicates n = 4), were randomly divided in the treatment groups in a *matched pairs* design as described in Yadetie et al. (2018). The same design was used in experiment II (mixture exposure) using four (one female and three male) fish. Exposure groups are hereafter referred to as either PFOS, PFOA, PFNA or Mix combined with their respective exposure concentrations (*e.g.*, PFOS100, Mix50 *etc.*) (Table 1). After 48 h of exposure, the slices were weighed, snap-frozen in liquid nitrogen, and stored at −80 °C for further analyses, or applied directly in viability analysis.

2.3. MTT assay - viability

The viability of the PCLS was assessed using the MTT assay, described in detail in Yadetie et al. (2018). Briefly, individual slices were rinsed in cold PBS, incubated in ice-cold MTT solution (2 mg/mL dissolved in L15-medium) for 90 min with shaking (10 °C, 50 rpm), rinsed again with PBS and incubated with DMSO (100%) for 20 min (room temperature, 50 rpm). Triplicates of 100 μL per well were transferred to a 96-well plate and subjected to absorbance measurements at 590 nm using an Enspire plate reader (Perkin Elmer, Waltham, MA, USA).

Table 1
Exposure setup and PFAS concentrations (μM).

Experiment	Control (DMSO 0.1%)	Exposure concentration (μM)		
		10	50	100
I. Single compound exposure groups	DMSO_s	PFOS10	PFOS50	PFOS100
		PFOA10	PFOA50	PFOA100
		PFNA10	PFNA50	PFNA100
II. Mixture exposure groups[a]	DMSO_m	Mix10	Mix50	Mix100

[a] The indicated concentrations of the mixtures are for each of the components PFOS, PFOA and PFNA.

2.4. RNA extraction

For each of the two experiments (single compound and mixture exposure), total RNA was extracted from frozen liver slices (four slices per group from four individual fish, n = 4) using the TRI Reagent User Guide (Thermo Fisher Scientific, Waltham, MA, USA). The concentration of the extracted RNA was determined using the NanoDropTm One MicroVolume UV–Vis Spectrophotometer (Thermo Fisher Scientific).The 260/280 nm absorbance ratios were > 1.85, and the 260/230 absorbance ratios were > 1.80 for all samples. RNA quality was assessed using agarose gel electrophoresis and an Agilent 2100 Bioanalyzer (Agilent Technologies, Santa Clara, CA, USA) for RNA-seq samples. All samples had RNA integrity numbers (RIN) > 8.9.

2.5. RNA sequencing, read mapping and differential expression analysis (DEA)

RNA samples from the PFAS exposures were submitted to Novogene (Cambridge, UK) for sequencing. Per sample, about 20 million 150 bp paired-end reads were generated using the Illumina NovaSeq 6000 system. Analysis of RNA seq data was performed as described in Yadetie et al. (2018), applying the RASflow analysis workflow (Zhang and Jonassen, 2020) with the Atlantic cod reference genome (GadMor3) downloaded from the Ensembl database (www.ensembl.org). Prior to differential expression analysis (DEA), genes with counts per million (CPM) <1 were filtered out. After DEA, differentially expressed genes (DEGs) were generated using the following cut-offs: Fold change (FC) >1.5 or < 0.67 (for up- or down-regulated genes, respectively) and false discovery rate (FDR) < 0.05.

2.6. Hierarchical clustering and principal component analysis

Hierarchical clustering (using average linkage method) and principal component analysis (PCA) were performed in Qlucore Omics Explorer version 3.4 (Qlucore AB, Lund, Sweden), using log2-transformed normalized expression values of all genes in individual samples. The top discriminating genes as filtered by FDR q-values (within-subjects ANOVA) were represented in clustering and PCA plots.

2.7. Pathway and gene set enrichment analysis

Pathway analysis was performed as described in Yadetie et al. (2018) using human orthologs of Atlantic cod genes retrieved from the Ensembl database (www.ensembl.org). For pathway and network enrichment analysis of DEGs, the tools and databases including the ClueGO application in Cytoscape (Bindea et al., 2009) and Enrichr (Kuleshov et al., 2016) were used with default settings unless specified otherwise. Gene set enrichment analysis (GSEA) was performed using the GSEA software (https://www.gsea-msigdb.org), with the following settings: The Hallmark gene set database (Liberzon et al., 2015) was applied, the tTest metric for ranking was utilized, and for significant enrichment, the default FDR < 0.25 was applied (Subramanian et al., 2005).

2.8. Statistical test for non-additive mixture effects

To test for genes with non-additive mixture effects, we used the DEGs list from the Mix100 exposure as basis for the analysis. A mixture effect was defined as additive if the log fold change was equal to the prediction:

$$\log_2(FC_{mixture}) = \log_2(FC_{PFOS}) + \log_2(FC_{PFOA}) + \log_2(FC_{PFNA})$$

An observed mixture value below or above this additive prediction is said to be antagonistic or synergistic, respectively (Groten et al., 2001). We applied the expression values for the highest concentration of each

single PFAS exposure (100 μM) and compared the prediction with the actual expression values for the Mix100 (containing 100 μM of each compound) exposure. For each gene, we fitted two linear models to the $\log_2$ (FC) data. The first model is purely additive, while the second one has an additional interaction term. To test if the two models were different, we performed an ANOVA (Casella and Berger, 2002). This gave a *p*-value for each gene, where a low *p*-value corresponds to a strong non-additive mixture effect. Due to the high number of tests ($n = 733$), the *p*-values were corrected for multiple testing. This was done using the method of Holm (1979) which increases the *p*-values such that a fixed significance level can be used independent of the number of tests.

3. Results

3.1. PCLS viability

MTT assays were performed with slices from each treatment to assess the viability of liver slices following 48 h of PFAS exposure. No significant changes in viability were observed in any of the PFAS-exposed groups compared to the DMSO control (Supplementary Fig. S1).

3.2. Differentially expressed genes (DEGs) following PFAS exposure

There were differences among single PFAS, and also between single PFAS and the mixtures, in the number of DEGs following exposure (Table 2, Supplementary Table S2). Among single PFAS, PFOS exposure produced the highest number of unique DEGs (86), compared to PFOA and PFNA, whose exposure generated 25 and 31 unique DEGs, respectively. Several of the DEGs related to PFOA and PFNA exposure were common with DEGs related to PFOS exposure (Fig. S2). Compared to single PFAS, mixture exposure (Table 2) generated a larger number of unique DEGs (841).

3.3. Hierarchical clustering and principal component analysis following PFAS exposure

To study the differences in expression profiles between single PFAS and the mixtures, normalized counts of RNA-seq data from all exposures were subjected to hierarchical clustering analysis and PCA. Based on ANOVA ($p < 1.52e\text{-}04$, $q < 0.01$), the top 169 discriminating genes are highlighted in the cluster analysis (Fig. 1A). The Mix100 exposure group provoked the largest difference in expression pattern compared to the DMSO control, followed by PFOS100, suggesting that PFOS contributes to a large part of the effects following mixture exposure. This is also reflected in the PCA plot (Fig. 1B), where PFOS100 clusters closer to Mix100 compared to the other exposure groups. Furthermore, among annotated DEGs from the list in Table 2, 40 of 52 DEGs in the PFOS exposure are also shared with DEGs in the mixture (Fig. S3). The lowest exposure concentrations (10 μM) of each compound were excluded from Fig. 1 to enhance visualization (all groups are presented in Supplementary Fig. S4), but were run in a separate analysis. Interestingly, PFNA10 produced a higher number of DEGs both compared to the other single compounds and to Mix10 (Table 2, listed in Supplementary Table S2). Furthermore, PFNA10 tended to separate from the other groups both in hierarchical clustering and PCA, suggesting low dose effects (Supplementary Fig. S5A), although this was not statistically significant.

3.4. Enriched gene sets obtained with GSEA following PFAS exposure

Due to the relatively low number of DEGs following single PFAS exposure, we applied GSEA which may identify gene sets enriched from moderate gene expression changes (Subramanian et al., 2005). For PFOS100, GSEA identified one significantly enriched pathway (FDR *q*-value <0.25), the REACTIVE_OXYGEN_SPECIES pathway (Fig. 2A). The genes involved in the core enrichment of this gene set show higher expression in the PFOS-exposed liver slices compared to the DMSO control (Fig. 2B). No gene sets were found to be significantly enriched following exposure to PFOA100 or PFNA100 (Table S3).

Table 2
Number of differentially expressed genes (DEGs) in Atlantic cod PCLS following 48 h PFAS exposure. The following cut-offs were applied to generate DEGs: Fold change (FC) > 1.5 or < 0.67, log counts per million (log CPM) > 0 and false discovery rate (FDR) < 0.05. Detailed information of DEGs is found in Table S2.

Concentration (μM)	10	50	100	Sum unique DEGs[a]
PFOS	6	8	74	86
PFOA	4	6	18	25
PFNA	13	7	15	31
Mix	9	96	812	841

[a] The sum of unique DEGs excludes identical DEGs among different concentrations for the same compound/mixture.

GSEA was also applied for the Mix50 and Mix100 exposure groups. No gene sets were significantly enriched following exposure to Mix50 (data not shown). For Mix100, GSEA revealed three significantly (FDR q-value <0.25) enriched gene sets, namely the REACTIVE_OXYGEN_SPECIES, MTORC1_SIGNALING, and UNFOLDED_PROTEIN_RESPONSE pathways (Fig. 3). The core enrichment genes within these gene sets were mostly up-regulated compared to the DMSO control. Examples of up-regulated genes included the glutathione cysteine ligase catalytic and modifier unit (*gclc* and *gclm*, respectively) and peroxiredoxin 1 (*prdx1*), all of which were among the enriched genes in both the REACTIVE_OXYGEN_SPECIES and MTORC1_SIGNALING gene sets.

3.5. Pathway and network analysis following PFAS exposure

For pathway analysis, DEGs from all three concentrations (unique DEGs, Table 2) of each single PFAS were combined. For PFOS, significantly (FDR <0.05) enriched pathways were mostly related to nuclear receptor-related pathways, including the estrogen and farnesoid X receptor (Er/Fxr) pathways, in addition to cholesterol metabolism (Table 3). Within these pathways, important genes included estrogen receptor 1 (*esr1*), cytochrome P450 7a1 (*cyp7a1*), angiopoietin like 3 (*angptl3*), and apolipoprotein E (*apoe*). For PFOA, significantly (FDR < 0.05) enriched pathways were linked to biotransformation and metabolic processes of steroids and lipids (Table S4A). A few enriched pathways related to regulation of RNA polymerase II and protein localization were also observed following PFNA exposure (Table S4B).

DEGs from both the 50 and 100 μM mixture exposures were analysed separately in pathway analysis to investigate any concentration-dependent differences in affected pathways. Of the 53 annotated DEGs for Mix50, 42 were shared with Mix100 (Supplementary Fig. S6), suggesting a dose-response trend. Following Mix50 exposure, significantly enriched pathways (FDR < 0.05) using the Enrichr tool (Kuleshov et al., 2016) were related to fatty acid biosynthesis and metabolic pathways in cancer (Supplementary Table S5). An up-regulation of several genes essential for lipid biosynthesis, including ATP citrate lyase (*acly*) and fatty acid synthase (*fasn*), were responsible for enrichment of these pathways. Albeit not significant, the top two KEGG pathways for Mix50 exposure were similar to enriched pathways for Mix100 (ferroptosis, see below) and PFOS100 (cholesterol metabolism) exposure.

Following Mix100 exposure, pathway analysis revealed enrichment of pathways related to several cellular processes, including nuclear receptor and nuclear factor erythroid 2-related factor 2 (Nrf2) pathways, ferroptosis, and cancer-related pathways (Fig. 4). Most of the genes within the enriched pathways were up-regulated following mixture exposure.

3.6. Mixture effect analysis

To investigate the presence of interacting effects among the PFAS in the mixture, a mixture effect analysis was performed using the DEGs from the Mix100 exposure, by comparing a predicted gene expression level based on single compounds, with the actual expression level in the mixture. When comparing the predicted value and the measured expression in Mix100, 71 of 733 genes from the DEGs list (Table 2) showed significant ($p < 0.05$) non-additive mixture effects (Fig. 5). This means that 662 of the 733 genes (90%) did not show significant non-additive effects and were well described by the additive

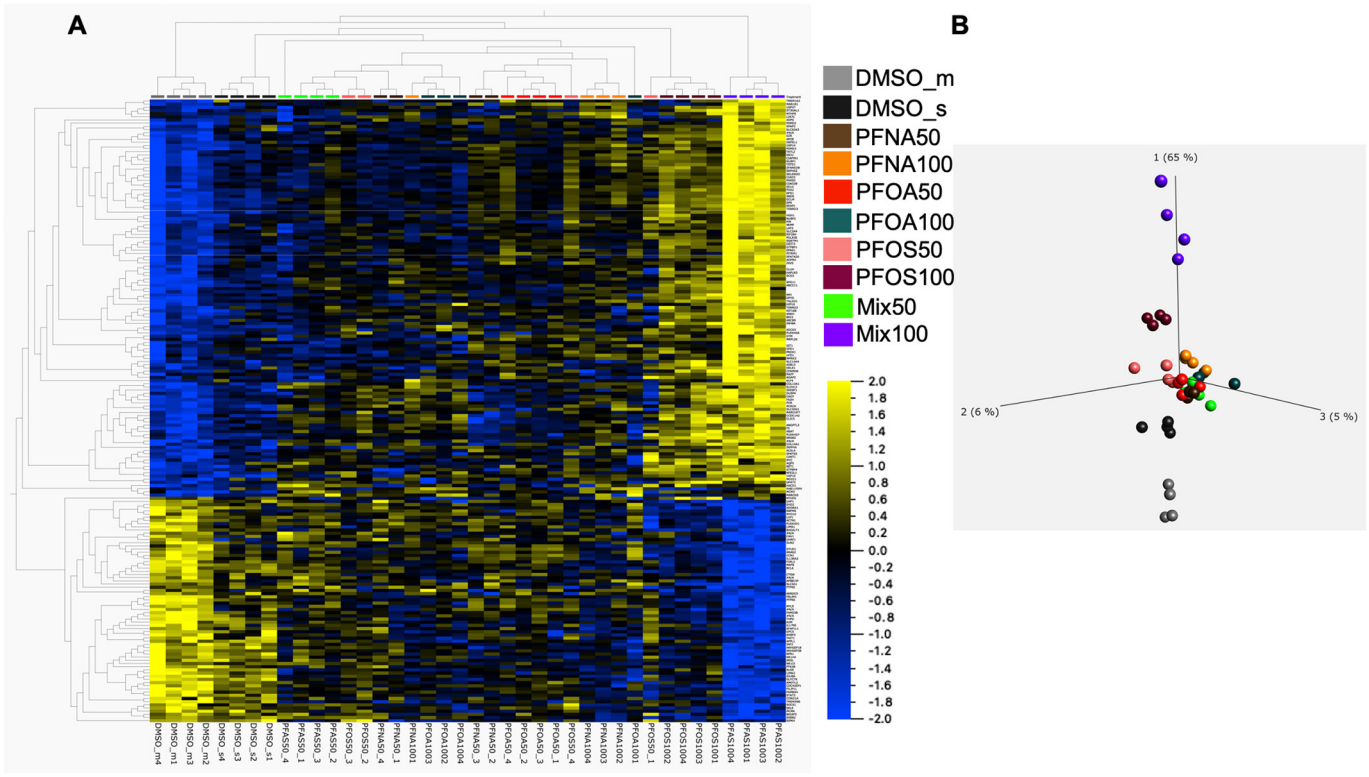

Fig. 1. Two-way hierarchical clustering and principal component analysis (PCA) of genes in PCLS samples of Atlantic cod exposed to single PFAS and the PFAS mixtures. Data represent expression values (log-transformed) of 169 top discriminating genes (ANOVA, $p < 1.52e\text{-}04$, q-value <0.01). The heatmap (A) shows relative expression levels as shown by the colour scale (middle bottom), with yellow and blue ends representing highest and lowest relative expression, respectively. Rows represent genes and columns represent samples. Controls (DMSO_s for single PFAS and DMSO_m for the mixtures) and exposure groups (PFOS, PFOA, PFNA, and Mix, with concentrations 50 and 100 μM) are indicated by the colour legend (middle top). The three first principal components in the PCA (B) represents 76% of the variance.

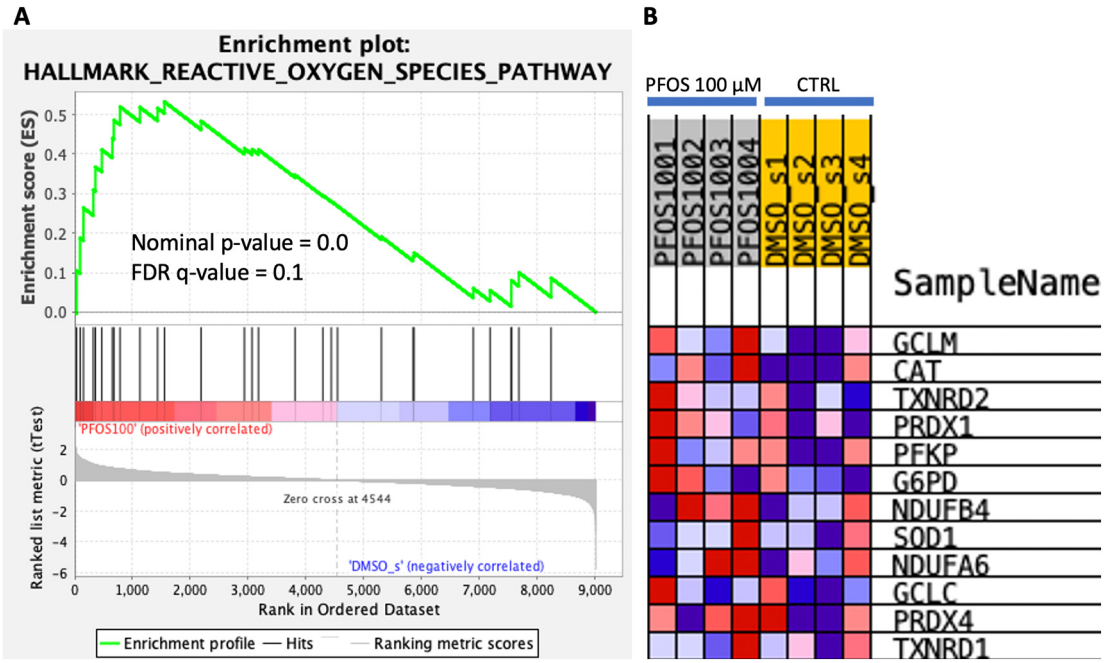

Fig. 2. Enrichment plot of the REACTIVE_OXYGEN_SPECIES pathway (A) and the corresponding core enrichment genes (B) in PCLS of cod exposed to PFOS (100 μM) *versus* control (DMSO) analysed with GSEA. Data represent log2-transformed gene expression values in control (DMSO_s) and high dose PFOS (100 μM) exposed samples. The heatmap (B) represents gene expression levels, with red and blue representing high and low relative expression, respectively.

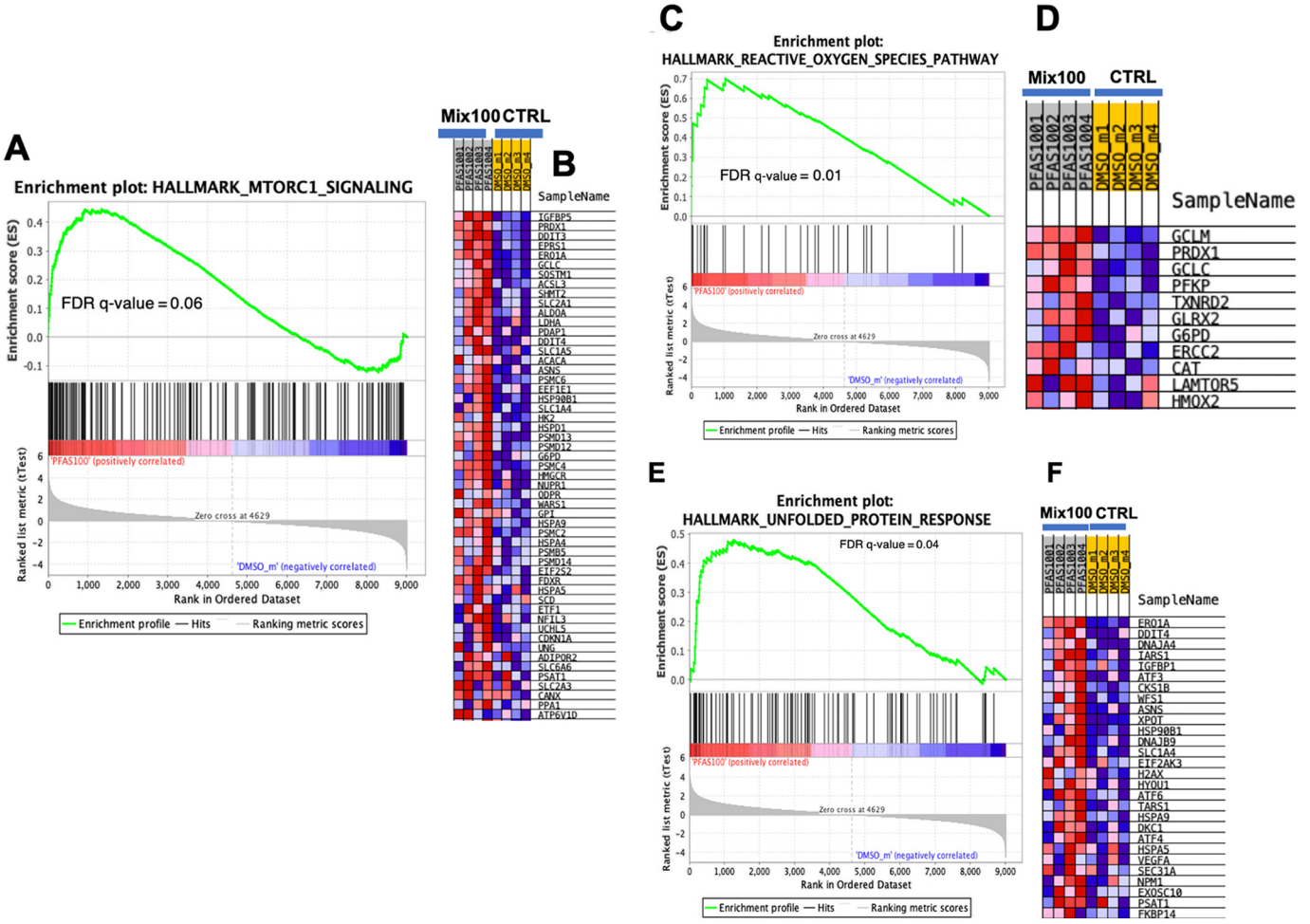

Fig. 3. Enrichment plots and core-enriched genes in PCLS of cod exposed to a PFAS mixture (100 μM) *versus* control (DMSO) analysed with GSEA. Data represent log2-transformed normalized gene expression values in control (DMSO_m) and high dose of PFAS mixture (100 μM) exposed samples. Enrichment plots of the significantly enriched pathways MTORC1_SIGNALING (A), REACTIVE_OXYGEN_SPECIES (C) and UNFOLDED_PROTEIN_RESPONSE (E) are presented with their corresponding heatmaps (B, D, F, respectively) representing gene expression levels of core enrichment genes, where red and blue corresponds to high and low relative expression, respectively.

model. Of the 71 genes with non-additive effects, a majority of 52 genes showed synergistic effects. Examples of genes with synergistic expression in the mixture include the antioxidant *prdx1* and *prdx5*, genes encoding transport proteins such as solute carriers (*slc*) and ATP binding cassette (*abc*) transporters, and some genes encoding transmembrane proteins (*tmem*, *tmtc*).

4. Discussion

4.1. PFOS exposure induces greater transcriptomic effects in PCLS compared to PFOA and PFNA exposure

The present study investigated transcriptomic responses of Atlantic cod PCLS exposed to PFAS, including both single compounds and three PFAS mixtures. Among single PFAS, PFOS exposure resulted in differential expression of a greater number of genes compared to PFOA and PFNA (Table 2, Supplementary Table S2). These dissimilarities in transcriptomic effects between PFAS may be linked to differences either in chemical uptake or toxic potential. Generally, it is observed that the bioaccumulation potential of PFAS increases with increasing carbon backbone length, but also that PFSAs bioaccumulate to a higher extent compared to PFCAs (Conder et al., 2008; Liu et al., 2019; Martin et al., 2003). In zebrafish (*Danio rerio*), a higher bioconcentration factor (BCF) was determined for PFOS (BCF = 2700) compared to PFOA (100) and PFNA (610) following six days of exposure (Menger et al., 2020). Also, PFOS concentrations in Atlantic salmon (*Salmo salar*) liver were three-four times higher compared to PFOA concentrations following two days of feed exposure (Mortensen et al., 2011), which is a similar exposure duration compared to this study. Moreover, some studies suggest that PFOS is more toxic compared to PFOA and PFNA. PFOS was found to be more potent in provoking developmental toxicity compared to PFNA and PFOA in zebrafish embryos (Zheng et al., 2012). Furthermore, PFOS toxicity was 2–100 times greater compared to PFOA for different endpoints and at several trophic levels, especially for turbot (*Psetta maxima*) embryos and larvae (Mhadhbi et al., 2012). However, in a study on gene expression profiles following exposure of cultured hepatocytes of rare minnow (*Gobiocypris rarus*), PFOA exposure gave a higher number of DEGs compared to PFOS exposure (Wei et al., 2009). Together, these findings suggest that toxicity of single PFAS may vary depending on factors such as chosen endpoint, developmental stage, species, *etc.* Still, variations in accumulative and toxic potential for individual PFAS may have caused the observed differences in DEGs in our study.

Following PFOA and PFNA exposure alone, a relatively low number of DEGs were generated (Table 2), and few pathways were significantly affected (Supplementary Table S4). Several of the DEGs generated following PFOA and PFNA exposure (43 and 50%, respectively) were also significantly expressed following PFOS exposure (Supplementary Fig. S2). Therefore, we will focus primarily on effects following PFOS exposure among effects produced by single PFAS. Using GSEA, we found that the REACTIVE_OXYGEN_SPECIES pathway was significantly enriched following exposure to PFOS100 (Fig. 2). Enrichment of this gene set was also observed following mixture exposure,

Table 3
Significantly (false discovery rate < 0.05) enriched pathways (WikiPathways, KEGG and Gene Ontology Biological Process) following exposure of cod PCLS to PFOS. Genes are colored red or green for indicating increased (FC > 1.5) or decreased (FC < 0.67) expression, respectively.

WikiPathways 2021

Term	Adj. p-val	Genes
Estrogen Receptor Pathway WP2881	5,12E-04	PCK1,NR0B2,ESR1
Nuclear Receptors Meta-Pathway WP2882	9,49E-03	SLC5A12,PCK1,GCLM,CYP7A1,NR0B2,ESR1
Farnesoid X receptor pathway WP2879	4,04E-02	NR0B2,CYP7A1

KEGG Pathways 2021

Term	Adj. p-val	Genes
Cholesterol metabolism	2,68E-02	ANGPTL3,APOE,CYP7A1
Thiamine metabolism	3,07E-02	THTPA,NFS1

Gene Ontology (Biological Process) 2021

Term	Adj. p-val	Genes
sterol metabolic process (GO:0016125)	3,30E-04	ANGPTL3,FDX2,APOE,CYP7A1,NR0B2
cholesterol metabolic process (GO:0008203)	1,10E-02	ANGPTL3,APOE,CYP7A1,NR0B2
regulation of developmental growth (GO:0048638)	1,33E-02	AGR2,NRCAM,APOE
secondary alcohol metabolic process (GO:1902652)	1,33E-02	ANGPTL3,APOE,NR0B2
regulation of extent of cell growth (GO:0061387)	1,49E-02	NRCAM,APOE
positive regulation of angiogenesis (GO:0045766)	1,66E-02	HSPB6,WNT5A,KDR,ANGPTL3
positive regulation of vasculature development (GO:1904018)	1,66E-02	HSPB6,WNT5A,KDR,ANGPTL3
sterol catabolic process (GO:0016127)	1,95E-02	APOE,CYP7A1
cholesterol catabolic process (GO:0006707)	1,95E-02	APOE,CYP7A1
regulation of neuron projection development (GO:0010975)	1,95E-02	WNT5A,KNDC1,APOE,ITM2C
positive regulation of tumor necrosis factor secretion (GO:1904469)	2,25E-02	C1QTNF4,WNT5A
alcohol catabolic process (GO:0046164)	2,25E-02	APOE,CYP7A1
cholesterol homeostasis (GO:0042632)	2,48E-02	ANGPTL3,APOE,CYP7A1
sterol homeostasis (GO:0055092)	2,48E-02	ANGPTL3,APOE,CYP7A1
regulation of tumor necrosis factor secretion (GO:1904467)	3,42E-02	C1QTNF4,WNT5A
anion homeostasis (GO:0055081)	4,41E-02	ANGPTL3,APOE
regulation of endothelial cell proliferation (GO:0001936)	4,41E-02	WNT5A,KDR,APOE
regulation of angiogenesis (GO:0045765)	4,41E-02	HSPB6,WNT5A,KDR,ANGPTL3
organonitrogen compound biosynthetic process (GO:1901566)	4,41E-02	FA2H,NFS1,ELOVL3,INHBA
phosphate-containing compound metabolic process (GO:0006796)	4,41E-02	THTPA,DUSP4,ANGPTL3,PLB1
GTP metabolic process (GO:0046039)	4,41E-02	NFS1,GTPBP1
cellular response to hexose stimulus (GO:0071331)	4,41E-02	PCK1,CYP7A1
positive regulation of lipid metabolic process (GO:0045834)	4,41E-02	ANGPTL3,APOE
acylglycerol homeostasis (GO:0055090)	4,64E-02	ANGPTL3,APOE

and its implications are discussed in more detail below. In addition, significantly enriched pathways involving DEGs related to PFOS exposure included nuclear receptor pathways and metabolism of sterols such as cholesterol (Table 3). PFAAs have been shown to alter receptor pathways such as aryl hydrocarbon receptor (Ahr), peroxisome proliferator activated receptor (Ppar), and retinoid X receptor (Rxr), in addition to affecting genes related to xenobiotic metabolism (summarized in Lee et al., 2020). Furthermore, the significant enrichment of the Fxr pathway (Table 3) may be linked to the enrichment of cholesterol metabolism pathways, as this receptor is essential for regulating cholesterol homeostasis (Lambert et al., 2003). Changes in genes contributing to the enrichment of cholesterol and sterol metabolism pathways were down-regulation of *cyp7a1*, and up-regulation of *angptl3* and *apoe*. Cyp7a1 catalyzes a rate-limiting step in cholesterol catabolism and bile acid synthesis (Post et al., 2006), suggesting that a down-regulation of this enzyme may increase cholesterol levels. Angptl3 is involved in regulating plasma lipid levels (Tikka and Jauhiainen, 2016), whereas Apoe is important in lipid transport and for catabolism of lipids and lipoproteins (Marais, 2019). Previous studies have also observed changes in expression of these genes following PFAS exposure. Both PFOS and PFOA have been shown to decrease *CYP7A1* expression in human HepaRG hepatoma cells (Behr et al., 2020), and increase cholesterol levels in Atlantic salmon larvae (Arukwe et al., 2013). Similar to the present study, PFOS induced apoe expression in zebrafish embryos (Fai Tse et al., 2016). In contrast, *apoe* expression was down-regulated following PFOS exposure in liver of common carp (*Cyprinus carpio*) (Hagenaars et al., 2008). Nevertheless, changes in expression of these metabolism-regulating genes suggest a modification of metabolic capacity in cod PCLS following PFOS exposure.

4.2. The PFAS mixtures affect metabolism pathways and stress responses in cod PCLS

Exposure of PCLS to the PFAS mixtures produced a higher number of DEGs in the transcriptome compared to single PFAS (Table 2), which may be expected due to a higher exposure load in the mixtures. Interestingly, the PFOS100 and Mix100 exposure groups clustered closer together compared to the other exposure groups (Fig. 1), indicating that effects on transcriptomic responses following mixture exposure may largely be mediated

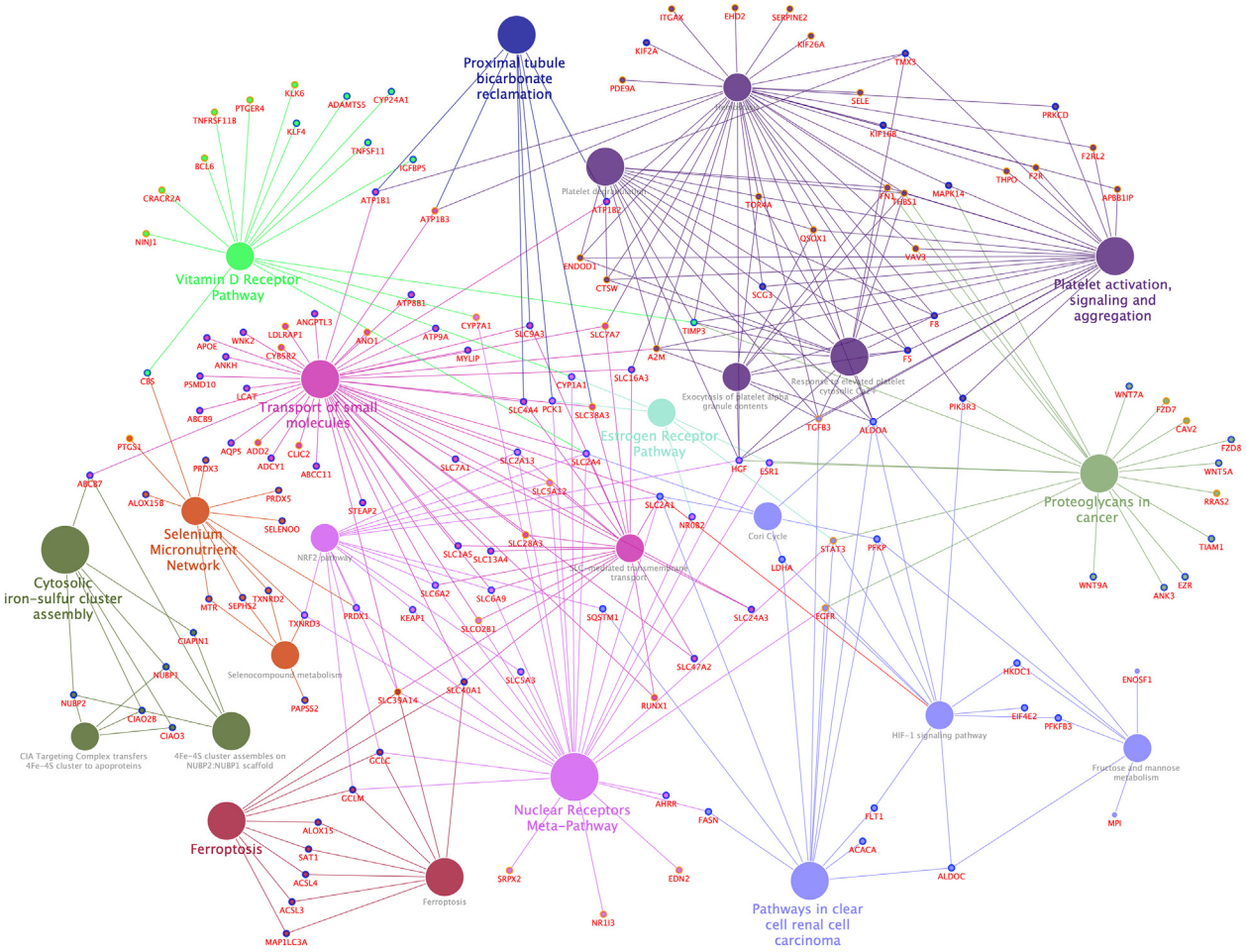

Fig. 4. Cytoscape ClueGo networks showing DEGs and enriched pathways in cod PCLS exposed to 100 μM PFAS mixture. Significantly enriched networks (Bonferroni step-down correction, adjusted *p*-value <0.05) generated using ClueGo with Wikipathway, KEGG and Reactome databases are shown. Pathway-terms with at least 50% shared genes have same group color for the nodes, edges, and the name of the most significant term. The size of a pathway-term node is proportional to the number of constituent DEGs. Gene symbols are shown in red, and the outer edge of the gene nodes are colored blue and orange for up- and down-regulated genes, respectively.

by PFOS. This observation is in line with the suggestion above that PFOS may either accumulate to a higher extent and/or be more toxic to PCLS compared to PFOA and PFNA. Another study also found that toxicity of a binary mixture of PFOS and PFOA increased with increasing molar ratio of PFOS compared to PFOA in zebrafish embryos (Ding et al., 2013).

Significantly enriched pathways following mixture exposure were mainly related to stress responses. Using GSEA, the REACTIVE_OXYGEN_SPECIES pathway was, similar to PFOS100 exposure, significantly enriched also for Mix100 (Fig. 3C, D), and pathway analysis highlighted the nuclear receptor and the Nrf2 pathways as significantly enriched, among others (Fig. 4). These pathways are interlinked through common genes and are related to cellular and oxidative stress responses. Nrf2 is a transcription factor essential for regulating several antioxidant and phase II biotransformation genes in vertebrates through interactions with antioxidant response elements (AREs) present in the promotor region of these genes (Timme-Laragy et al., 2012). Some of the genes regulated through Nrf2 were among the core-enrichment genes in the GSEA of PFOS100 (Fig. 2) and/or Mix100 exposure (Fig. 3B) and were also highlighted in the pathway analysis following Mix100 exposure (Fig. 4). These genes included *gclc*, *glcm*, *prdx1*, thioredoxin reductase (*txnrd*) and glucose-6-phosphate dehydrogenase (*g6pd*) (Kensler et al., 2007). Within the core-enrichment genes were also other important antioxidant enzymes, including catalase (*cat*) and superoxide dismutase (*sod*), responsible for neutralizing superoxide radicals and hydrogen peroxide, respectively. Responses of antioxidant enzymes to contaminant exposure is complex; environmental contaminants may both induce or inhibit these enzymes (Benedetti et al., 2015; Dale et al., 2017). In this study, PFAS exposure largely induced the components of the antioxidant systems, which is in line with our previous *in vivo* study, where we observed an increase in enzyme activities of Cat and glutathione S-transferase (Gst) following PFAS exposure (Dale et al., 2020). Oxidative stress is well-established as a non-organ directed toxicity following exposure to PFAAs (Lee et al., 2020), and has been widely reported both in fish and other species. Nrf2 pathway-related genes were also induced by PFOS exposure in zebrafish (Sant et al., 2018), and by PFOA exposure in frog (*Rana nigromaculata*) (Tang et al., 2018). PFOS and PFOA significantly increased Cat and Sod activity, but reduced Gst activity, in cultured hepatocytes of tilapia (*Oreochromis niloticus*) (Liu et al., 2007). Additionally, crosstalk between Nrf2 and other transcription factor pathways, such as Ahr and Ppar signaling, may occur (Rousseau et al., 2015; Sant et al., 2018), which appears consistent with our results as nuclear receptor pathways were found to be enriched alongside Nrf2 following Mix100 exposure (Fig. 4).

Other oxidative stress-related pathways significantly enriched following Mix100 exposure were ferroptosis (Fig. 4) and the MTORC1_signalling and UNFOLDED_PROTEIN_RESPONSE gene sets (Fig. 3). The unfolded protein response is a protective response of the endoplasmic reticulum following diverse cellular stress signals, including oxidative stress (Chaudhari et al., 2014). Ferroptosis is an iron-dependent, non-apoptotic cell death process, provoked by lipid peroxidation. Induction of this response depends on changes in several biological processes, where excessive uptake of iron and increased synthesis of oxidized polyunsaturated fatty-acid containing phospholipids (PUFA-PLs) are linked to pro-ferroptosis (Tarangelo and Dixon, 2019). One of the key

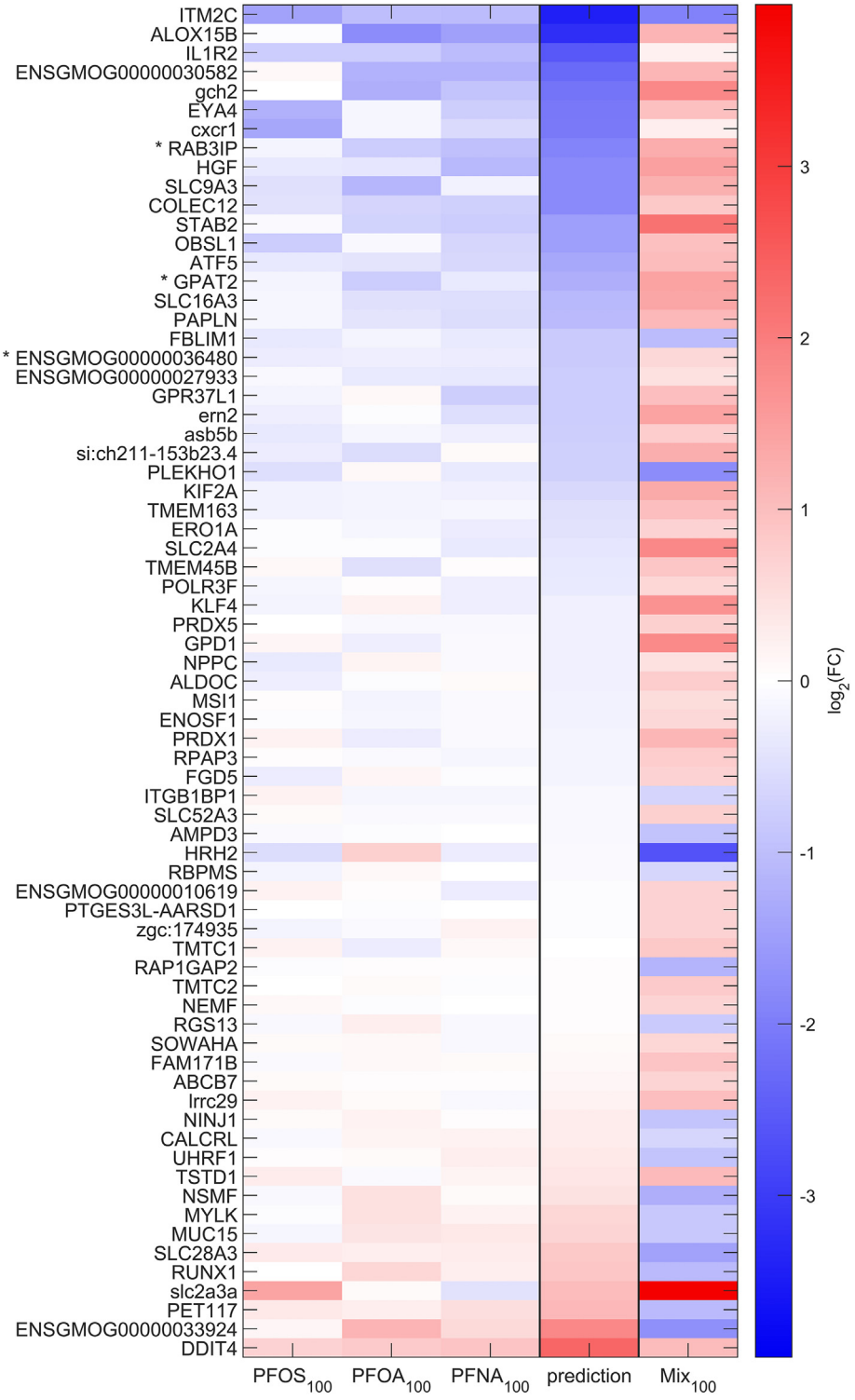

Fig. 5. Mixture effect analysis for the 100 μM PFAS exposures. Gene expression is presented as mean log fold change values. The first three columns are the observed values for the single PFAS exposures. The prediction column is the sum of the single PFAS columns and is the theoretical value if there is a purely additive mixture effect. The mixture column is the observed values for the mixture, and non-additive mixture effects can be identified as differences from the prediction column. Genes in this list were considered differentially expressed and their tests for non-additive mixture effects had a *p*-value below 0.05 before correction for multiple testing. The genes are sorted based on predicted values. An asterisk (*) indicates $p < 0.05$ after correcting for multiple testing. Human (capitalized) or zebrafish (small letter) gene names are presented, and where no human or zebrafish annotation were available, Atlantic cod ENSEMBL ID is applied.

enzymes of PUFA-PL synthesis is acyl coenzyme-A synthetase long-chain family member 4 (Acsl4), whose gene was found to be significantly up-regulated following Mix100 (Fig. 4). Moreover, the mechanistic target of rapamycin complex 1 (mTORC1) is thought to be a regulator of ferroptosis by inhibiting pro-ferroptotic pathways and thus protecting cells against ferroptosis (Lei et al., 2021). Additionally, the glutathione biosynthesis pathway, where *gclm* and *gclc* are important genes encoding the glutamate cysteine ligase enzyme, is known to be anti-ferroptotic. The prevention of ferroptosis by the glutathione redox system has been deemed essential in clear cell renal carcinoma (Miess et al., 2018), another pathway found to be significantly enriched in

our study (Fig. 4). Based on the observed enrichment of the above-mentioned pathways, we may propose ferroptosis as a possible adverse outcome of PFAS exposure. Ferroptosis is also listed as a significantly affected pathway in recent publications investigating effects of PFAS exposure in mice (Pfohl et al., 2020; Rashid et al., 2020). However, to our knowledge, there currently exists no research linking PFAS exposure to the ferroptosis pathway in teleosts.

Pathway analyses were also performed with the Mix50 exposure group. 42 of the 53 annotated DEGs for Mix50 exposure were shared with the Mix100 exposure group (Supplementary Fig. S6), supporting a dose-dependent effect on transcriptomic responses, where Mix100 induced the same pathways, but also several others. However, the pathways induced by Mix100 were to a higher degree related to stress-responses compared to Mix50 exposure, where enriched pathways included lipid and fatty acid biosynthesis and metabolism (Supplementary Table S5). This finding may be explained by the larger exposure load in the Mix100 group (100 μM of each compound), which is likely to increase the cellular stress within the liver slices, even though viability of the liver slices was apparently not reduced at 48 h (Supplementary Fig. S1).

4.3. Lack of effects on Ppara signaling pathway following PFAS exposure

The detailed mechanism of how PFAS induce oxidative stress remains to be determined. However, effects on fatty acid oxidation, *e.g.* β-oxidation, is suggested as a possible pathway through which PFAS-induced oxidative stress is mediated (Lee et al., 2020). β-oxidation is controlled by activation of the Ppara signaling pathway (Olivares-Rubio and Vega-López, 2016). There are conflicting findings regarding the ability of PFAS to activate Ppars in fish (Arukwe and Mortensen, 2011; Ren et al., 2009; Sant et al., 2021; Söderström et al., 2022). We have recently reported effects on the Ppara signaling pathway, specifically an induction of fatty acid β-oxidation accompanied by a decrease in triglyceride levels, in liver of Atlantic cod exposed *in vivo* to a similar PFAS mixture (Dale et al., 2020). Therefore, we investigated whether genes related to this pathway were affected by PFAS exposure in PCLS. In this study, however, Ppara signaling and fatty acid β-oxidation were not among the significantly enriched pathways. In our previous *in vivo* study, Atlantic cod were exposed through intraperitoneal injections to PFAS for two weeks, with one week between the final injection and sampling. Also, the concentrations of PFAS were lower (environmentally relevant) compared to this study. The lack of effects on fatty acid β-oxidation might be related to some of these differences. Other researchers have observed similar differences in the ability of PFAS (in this case PFOA) to affect β-oxidation, where induction of this pathway was seen following 28 days of *in vivo* exposure (Wei et al., 2008), but not following 48 h of exposure in cultured hepatocytes of rare minnow (Wei et al., 2009). In contrast, a significant upregulation of *ppara* and the rate-limiting enzyme of peroxisomal β-oxidation, acyl coenzyme A-oxidase 1 (*acox1*) was observed in liver of Atlantic salmon (*Salmo salar*) following two days of feed exposure to PFAS (Arukwe and Mortensen, 2011). Although the exposure duration here was similar to our study, the exposure route, concentrations, and model species were not. Furthermore, there may also be structural differences among the ability of PFAS to act as Ppara agonists in Atlantic cod. Studies from our lab have shown (using luciferase reporter assays) that the carboxylated PFOA and PFNA activate Atlantic cod Ppara, which is not the case for the sulfonated PFOS (Söderström et al., 2022), a finding which has also been observed with mouse PPARA (Wolf et al., 2014). These findings are in line with the suggestion above that if PFOS has accumulated to a higher degree in the liver slices compared to PFOA and PFNA, it may account for the lack of enrichment of the Ppara signaling and β-oxidation pathways in this study.

4.4. Interacting effects of PFAS

Studying and understanding biological effects following exposure to PFAS mixtures is complex, as PFAS differ in their chemical structures, mode of action (MoA) and toxic potentials (McCarthy et al., 2021). Furthermore, as mentioned in the introduction several studies have shown interacting effects of PFAS in mixtures (Summarized in Ojo et al., 2021). In the present study, transcriptomic effects among the single PFAS were most prominent following PFOS exposure, but compared to single compounds, the mixture exposure produced a relatively large number of DEGs. The total exposure load is higher in the PFAS mixtures, which may partly explain the higher number of DEGs. However, this observation led us to investigate potential interactions among single PFAS within the 100 μM mixture (Mix100), by performing a simple analysis of non-additive mixture effects. We observed significant ($p < 0.05$) non-additive effects for almost 10% of the total number of DEGs from the Mix100 exposure (Fig. 5), where more-than-additive (synergistic) effects were observed for 52 of 71 genes. Examples of genes displaying synergistic responses were the antioxidant genes *prdx1* and *prdx5,* several membrane transport genes including *slc* and *abc* genes, and some genes encoding transmembrane-related proteins such as *tmem*s and *tmtc*s. Two previous studies observed both additive and more-than-additive effects on various cellular processes, including activation of Ppara, when investigating interactions among binary combinations of PFAAs (Ding et al., 2013; Wolf et al., 2014). Specifically, additivity was observed at lower concentrations, but tendencies of potentiation or synergism were observed at higher concentrations. With regards to synergistic effects on membrane-related components, other studies have indicated that PFAS, with their surfactant properties, may affect membrane permeability (Lee et al., 2020; Wei Liu et al., 2009; Rodea-Palomares et al., 2015). In addition, some studies have shown that PFAS may interact with Slc-related transporters, such as genes encoding the organic anion transporting polypeptides (*slco* or *oatp*) (Jantzen et al., 2016b; Jantzen et al., 2016a; Popovic et al., 2014). In humans and rats, these transporters may contribute to renal reabsorption of PFAS (Yang et al., 2010; Zhao et al., 2017). Although five *slc* transporters demonstrated a synergistic expression pattern, no Slco/Oatp-encoding genes were found in our gene lists, which may be attributed to factors such as tissue and/or species differences. Still, it is possible that interactions among single PFAS within the mixture cause synergistic effects on membrane-related processes such as permeability and transport, which may in turn affect PFAS uptake and/or clearance. A new experiment better designed to investigate interaction effects among the PFAS within the mixture (*e.g.*, by including several PFAS combinations with different concentrations and ratios) together with multivariate data analysis like partial least square regression (PLS) or isobologram, could aid our understanding of these possible interactions. Nevertheless, 90% of the DEGs from the mixture exposure showed additive expression patterns, suggesting that the main mixture effect in our study is additive.

4.5. Study limitations

Our results demonstrate the suitability of PCLS as a model system to study gene expression patterns in response to PFAS exposure using high throughput toxicogenomic approaches, which is in line with previous findings for other contaminants in both Atlantic cod (Yadetie et al., 2018) and Polar cod (*Boreogadus saida*) (Yadetie et al., 2021). However, the method has some limitations to be aware of. The region and depth of liver utilized to prepare slices, in addition to the presence of veins and bile ducts may affect the cellular composition within each slice, which in turn may yield differences in contaminant sensitivity (Eide et al., 2014). To avoid such differences, liver slices were randomized before being transferred to the well plates, and also, RNA extraction was performed from four pooled slice replicates. Paired-sample *t*-tests were applied to account for the relatively large variability observed in transcriptomic responses among individual fish. Finally, we did not measure accumulation of PFAS in the liver slices, and for future studies, a combination of chemical analysis with biological assays is desirable to increase our insights of accumulation and effects of PFAS in PCLS.

5. Conclusion

In this study, we have shown that PFAS exposure causes significant effects on transcriptomic responses in cod liver organ cultures, including effects on pathways related to sterol metabolism, nuclear receptors, and oxidative stress. Among single PFAS, PFOS seemed to cause greater effects compared to PFOA and PFNA, and PFOS also seemed to have an important

impact on significantly enriched pathways following exposure to the PFAS mixtures. The PFAS mixtures generated a higher number of DEGs compared to single PFAS exposure, and through analysis of non-additive effects in the Mix100 exposure group, we highlighted 52 and 19 genes with more-than-additive and less-than-additive effects, respectively. Although these findings are interesting to pursue, our analysis suggests that additivity is the main mixture effect following PFAS exposure.

Supplementary data to this article can be found online at https://doi.org/10.1016/j.scitotenv.2021.152732.

CRediT authorship contribution statement

Karina Dale: Conceptualization, Validation, Formal analysis, Investigation, Resources, Writing – original draft, Writing – review & editing, Visualization. **Fekadu Yadetie:** Methodology, Formal analysis, Investigation, Resources, Data curation, Writing – original draft, Writing – review & editing, Visualization. **Torill Horvli:** Validation, Formal analysis, Investigation, Resources, Writing – review & editing. **Xiaokang Zhang:** Formal analysis, Data curation, Writing – review & editing. **Håvard Guldbrandsen Frøysa:** Formal analysis, Writing – original draft, Writing – review & editing, Visualization. **Odd André Karlsen:** Conceptualization, Writing – review & editing, Supervision, Project administration, Funding acquisition. **Anders Goksøyr:** Conceptualization, Writing – review & editing, Supervision, Visualization, Project administration, Funding acquisition.

Declaration of competing interest

The authors declare that they have no known competing financial interests or personal relationships that could have appeared to influence the work reported in this paper.

Acknowledgements

This study was funded by the Research Council of Norway through the *dCod 1.0: decoding systems toxicology of Atlantic cod* project (Center for Digital Life Norway, project no. 248840) and the *iCod 2.0: Integrative environmental genomics of Atlantic cod* project (project no. 244564). The funding resources had no role in the design of the study and collection, analysis and interpretation of the data or writing of the manuscript.

References

Ahrens, L., 2011. Polyfluoroalkyl compounds in the aquatic environment: a review of their occurrence and fate. J. Environ. Monit. 13 (1), 20–31. https://doi.org/10.1039/C0EM00373E.

Ahrens, L., Bundschuh, M., 2014. Fate and effects of poly- and perfluoroalkyl substances in the aquatic environment: a review. Environ. Toxicol. Chem. 33 (9), 1921–1929. https://doi.org/10.1002/etc.2663.

Arukwe, A., Mortensen, A.S., 2011. Lipid peroxidation and oxidative stress responses of salmon fed a diet containing perfluorooctane sulfonic- or perfluorooctane carboxylic acids. Comp.Biochem.Physiol.C Toxicol.Pharmacol. 154 (4), 288–295. https://doi.org/10.1016/J.CBPC.2011.06.012.

Arukwe, A., Cangialosi, M.V., Letcher, R.J., Rocha, E., Mortensen, A.S., 2013. Changes in morphometry and association between whole-body fatty acids and steroid hormone profiles in relation to bioaccumulation patterns in salmon larvae exposed to perfluorooctane sulfonic or perfluorooctane carboxylic acids. Aquat. Toxicol. 130–131, 219–230. https://doi.org/10.1016/J.AQUATOX.2012.12.026.

Behr, A.-C., Kwiatkowski, A., Ståhlman, M., Schmidt, F.F., Luckert, C., Braeuning, A., Buhrke, T., 2020. Impairment of bile acid metabolism by perfluorooctanoic acid (PFOA) and perfluorooctanesulfonic acid (PFOS) in human HepaRG hepatoma cells. Arch. Toxicol. 94 (5), 1673–1686. https://doi.org/10.1007/s00204-020-02732-3.

Benedetti, M., Giuliani, M.E., Regoli, F., 2015. Oxidative metabolism of chemical pollutants in marine organisms: molecular and biochemical biomarkers in environmental toxicology. Ann. N. Y. Acad. Sci. 1340 (1), 8–19. https://doi.org/10.1111/nyas.12698.

Bindea, G., Mlecnik, B., Hackl, H., Charoentong, P., Tosolini, M., Kirilovsky, A., Fridman, W.-H., Pagès, F., Trajanoski, Z., Galon, J., 2009. ClueGO: a cytoscape plug-in to decipher functionally grouped gene ontology and pathway annotation networks. Bioinformatics (Oxford, England) 25 (8), 1091–1093. https://doi.org/10.1093/bioinformatics/btp101.

Boess, F., Kamber, M., Romer, S., Gasser, R., Muller, D., Albertini, S., Suter, L., 2003. Gene expression in two hepatic cell lines, cultured primary hepatocytes, and liver slices compared to the in vivo liver gene expression in rats: possible implications for toxicogenomics use of in vitro systems. Toxicol. Sci. 73 (2), 386–402. https://doi.org/10.1093/toxsci/kfg064.

Bopp, S.K., Barouki, R., Brack, W., Dalla Costa, S., Dorne, J.-L.C.M., Drakvik, P.E., Bergman, Å., 2018. Current EU research activities on combined exposure to multiple chemicals. Environ. Int. 120, 544–562. https://doi.org/10.1016/J.ENVINT.2018.07.037.

Bopp, S.K., Kienzler, A., Richarz, A.-N.N., van der Linden, S.C., Paini, A., Parissis, N., Worth, A.P., 2019. Regulatory assessment and risk management of chemical mixtures: challenges and ways forward. Crit. Rev. Toxicol. 49 (2), 174–189. https://doi.org/10.1080/10408444.2019.1579169.

Brockmeier, E.K., Hodges, G., Hutchinson, T.H., Butler, E., Hecker, M., Tollefsen, K.E., Falciani, F., 2017. The role of omics in the application of adverse outcome pathways for chemical risk assessment. Toxicol. Sci. 158 (2), 252–262. https://doi.org/10.1093/toxsci/kfx097.

Buck, R.C., Franklin, J., Berger, U., Conder, J.M., Cousins, I.T., de Voogt, P., Jensen, A.A., Kannan, K., Mabury, S.A., van Leeuwen, S.P., 2011. Perfluoroalkyl and polyfluoroalkyl substances in the environment: terminology, classification, and origins. Integr. Environ. Assess. Manag. 7 (4), 513. https://doi.org/10.1002/IEAM.258.

Casella, G., Berger, R., 2002. Statistical inference. Duxbury Advanced Series in Statistics And Decision Sciences, 2nd ed. Thomson Learning.

Cedergreen, N., 2014. Quantifying synergy: a systematic review of mixture toxicity studies within environmental toxicology. PloS One 9 (5), 96580. https://doi.org/10.1371/journal.pone.0096580.

Celander, M.C., 2011. Cocktail effects on biomarker responses in fish. Aquat. Toxicol. 105 (3), 72–77. https://doi.org/10.1016/j.aquatox.2011.06.002.

Chaudhari, N., Talwar, P., Parimisetty, A., Lefebvre d'Hellencourt, C., Ravanan, P., 2014. A molecular web: endoplasmic reticulum stress, inflammation, and oxidative stress. Front. Cell. Neurosci. 8, 213. https://doi.org/10.3389/fncel.2014.00213.

Conder, J.M., Hoke, R.A., de Wolf, W., Russell, M.H., Buck, R.C., 2008. Are PFCAs bioaccumulative? A critical review and comparison with regulatory criteria and persistent lipophilic compounds. Environ.Sci.Technol. 42 (4), 995–1003. https://doi.org/10.1021/es070895g.

Dale, K., Rasinger, J.D., Thorstensen, K.L., Penglase, S., Ellingsen, S., 2017. Vitamin E reduces endosulfan-induced toxic effects on morphology and behavior in early development of zebrafish (Danio rerio). Food Chem. Toxicol. 101, 84–93. https://doi.org/10.1016/j.fct.2017.01.004.

Dale, Karina, Yadetie, F., Müller, M.B., Pampanin, D.M., Gilabert, A., Zhang, X., Tairova, Z., Haarr, A., Lille-Langøy, R., Lyche, J.L., Porte, C., Karlsen, O.A., Goksøyr, A., 2020. Proteomics and lipidomics analyses reveal modulation of lipid metabolism by perfluoroalkyl substances in liver of Atlantic cod (Gadus morhua). Aquat. Toxicol. 227, 105590. https://doi.org/10.1016/J.AQUATOX.2020.105590.

Ding, G., Zhang, J., Chen, Y., Wang, L., Wang, M., Xiong, D., Sun, Y., 2013. Combined effects of PFOS and PFOA on zebrafish (Danio rerio) embryos. Arch. Environ. Contam. Toxicol. 64 (4), 668–675. https://doi.org/10.1007/s00244-012-9864-2.

Eide, M., Karlsen, O.A., Kryvi, H., Olsvik, P.A., Goksøyr, A., 2014. Precision-cut liver slices of Atlantic cod (Gadus morhua): an in vitro system for studying the effects of environmental contaminants. Aquat. Toxicol. 153, 110–115. https://doi.org/10.1016/j.aquatox.2013.10.027.

Fai Tse, W.K., Li, J.W., Kwan Tse, A.C., Chan, T.F., Hin Ho, J.C., Sun Wu, R.S., Chu Wong, C.K., Lai, K.P., 2016. Fatty liver disease induced by perfluorooctane sulfonate: novel insight from transcriptome analysis. Chemosphere 159, 166–177. https://doi.org/10.1016/J.CHEMOSPHERE.2016.05.060.

Groten, J.P., Feron, V.J., Sühnel, J., 2001. Toxicology of simple and complex mixtures. Trends Pharmacol. Sci. 22 (6), 316–322. https://doi.org/10.1016/S0165-6147(00)01720-X.

Hagenaars, A., Knapen, D., Meyer, I.J., van der Ven, K., Hoff, P., De Coen, W., 2008. Toxicity evaluation of perfluorooctane sulfonate (PFOS) in the liver of common carp (Cyprinus carpio). Aquat. Toxicol. 88 (3), 155–163. https://doi.org/10.1016/J.AQUATOX.2008.04.002.

Holm, S., 1979. Board of the Foundation of the Scandinavian Journal of Statistics A Simple Sequentially Rejective Multiple Test Procedure Author (s): Sture Holm Published by: Wiley on behalf of Board of the Foundation of the Scandinavian Journal of Statistics Stable U. Scand. J. Stat. 6 (2), 65–70.

Hylland, K., Tollefsen, K.E., Ruus, A., Jonsson, G., Sundt, R.C., Sanni, S., Røe Utvik, T.I., Johnsen, S., Nilssen, I., Pinturier, L., Balk, L., Baršiene, J., Marigòmez, I., Feist, S.W., Børseth, J.F., 2008. Water column monitoring near oil installations in the North Sea 2001–2004. Mar. Pollut. Bull. 56 (3), 414–429. https://doi.org/10.1016/j.marpolbul.2007.11.004.

Jantzen, C.E., Annunziato, K.A., Bugel, S.M., Cooper, K.R., 2016. PFOS, PFNA, and PFOA sublethal exposure to embryonic zebrafish have different toxicity profiles in terms of morphometrics, behavior and gene expression. Aquat. Toxicol. 175, 160–170. https://doi.org/10.1016/J.AQUATOX.2016.03.026.

Jantzen, C.E., Annunziato, K.M., Cooper, K.R., 2016. Behavioral, morphometric, and gene expression effects in adult zebrafish (Danio rerio) embryonically exposed to PFOA, PFOS, and PFNA. Aquat. Toxicol. 180, 123–130. https://doi.org/10.1016/j.aquatox.2016.09.011.

Kensler, T.W., Wakabayashi, N., Biswal, S., 2007. Cell survival responses to environmental stresses via the Keap1-Nrf2-ARE pathway. Ann. Rev. Pharmacol. Toxicol. 47 (1), 89–116. https://doi.org/10.1146/annurev.pharmtox.46.120604.141046.

Khan, E.A., Zhang, X., Hanna, E.M., Yadetie, F., Jonassen, I., Goksøyr, A., Arukwe, A., 2021. Application of quantitative transcriptomics in evaluating the ex vivo effects of per- and polyfluoroalkyl substances on Atlantic cod (Gadus morhua) ovarian physiology. Sci. Total Environ. 755, 142904. https://doi.org/10.1016/j.scitotenv.2020.142904.

Kuleshov, M.V., Jones, M.R., Rouillard, A.D., Fernandez, N.F., Duan, Q., Wang, Z., Koplev, S., Jenkins, S.L., Jagodnik, K.M., Lachmann, A., McDermott, M.G., Monteiro, C.D., Gundersen, G.W., Ma'ayan, A., 2016. Enrichr: a comprehensive gene set enrichment analysis web server 2016 update. Nucleic Acids Res. 44 (W1), W90–W97. https://doi.org/10.1093/nar/gkw377.

Lambert, G., Amar, M.J.A., Guo, G., Brewer, H.B., Gonzalez, F.J., Sinal, C.J., 2003. The Farnesoid X-receptor is an essential regulator of cholesterol homeostasis. J. Biol. Chem. 278 (4), 2563–2570. https://doi.org/10.1074/JBC.M209525200.

Lee, J.W., Choi, K., Park, K., Seong, C., Yu, S.Do, Kim, P., 2020. Adverse effects of perfluoroalkyl acids on fish and other aquatic organisms: a review. Sci. Total Environ. 707, 135334. https://doi.org/10.1016/J.SCITOTENV.2019.135334.

Lei, G., Zhuang, L., Gan, B., 2021. mTORC1 and ferroptosis: regulatory mechanisms and therapeutic potential. BioEssays April, 2100093. https://doi.org/10.1002/bies.202100093.

Liberzon, A., Birger, C., Thorvaldsdóttir, H., Ghandi, M., Mesirov, J.P., Tamayo, P., 2015. The Molecular Signatures Database (MSigDB) hallmark gene set collection. Cell Syst. 1 (6), 417–425. https://doi.org/10.1016/j.cels.2015.12.004.

Liu, C., Yu, K., Shi, X., Wang, J., Lam, P.K.S., Wu, R.S.S., Zhou, B., 2007. Induction of oxidative stress and apoptosis by PFOS and PFOA in primary cultured hepatocytes of freshwater tilapia (Oreochromis niloticus). Aquat. Toxicol. 82 (2), 135–143. https://doi.org/10.1016/J.AQUATOX.2007.02.006.

Liu, Wei, Zhang, Y.-B., Quan, X., Jin, Y.-H., Chen, S., 2009. Effect of perfluorooctane sulfonate on toxicity and cell uptake of other compounds with different hydrophobicity in green alga. Chemosphere 75 (3), 405–409. https://doi.org/10.1016/j.chemosphere.2008.11.084.

Liu, Wenxiu, Wu, J., He, W., Xu, F., 2019. A review on perfluoroalkyl acids studies: environmental behaviors, toxic effects, and ecological and health risks. Ecosyst.HealthSustain. 5 (1), 1–19. https://doi.org/10.1080/20964129.2018.1558031.

Marais, A.D., 2019. Apolipoprotein E in lipoprotein metabolism, health and cardiovascular disease. Pathology 51 (2), 165–176. https://doi.org/10.1016/J.PATHOL.2018.11.002.

Martin, J.W., Mabury, S.A., Solomon, K.R., Muir, D.C.G.G., 2003. Bioconcentration and tissue distribution of perfluorinated acids in rainbow trout (Oncorhynchus mykiss). Environ. Toxicol. Chem. 22 (1), 196–204. https://doi.org/10.1002/etc.5620220126.

McCarthy, C.J., Roark, S.A., Middleton, E.T., 2021. Considerations for toxicity experiments and risk assessments with PFAS mixtures. Integr. Environ. Assess. Manag. 17 (4), 697–704. https://doi.org/10.1002/ieam.4415.

Menger, F., Pohl, J., Ahrens, L., Carlsson, G., Örn, S., 2020. Behavioural effects and bioconcentration of per- and polyfluoroalkyl substances (PFASs) in zebrafish (Danio rerio) embryos. Chemosphere 245, 125573. https://doi.org/10.1016/J.CHEMOSPHERE.2019.125573.

Mhadhbi, L., Rial, D., Pérez, S., Beiras, R., 2012. Ecological risk assessment of perfluorooctanoic acid (PFOA) and perfluorooctanesulfonic acid (PFOS) in marine environment using Isochrysis galbana, Paracentrotus lividus, Siriella armata and Psetta maxima. J. Environ. Monit. 14 (5), 1375. https://doi.org/10.1039/c2em30037k.

Miess, H., Dankworth, B., Gouw, A.M., Rosenfeldt, M., Schmitz, W., Jiang, M., Saunders, B., Howell, M., Downward, J., Felsher, D.W., Peck, B., Schulze, A., 2018. The glutathione redox system is essential to prevent ferroptosis caused by impaired lipid metabolism in clear cell renal cell carcinoma. Oncogene 37 (40), 5435–5450. https://doi.org/10.1038/s41388-018-0315-z.

Mortensen, A.S., Letcher, R.J., Cangialosi, M.V., Chu, S., Arukwe, A., 2011. Tissue bioaccumulation patterns, xenobiotic biotransformation and steroid hormone levels in Atlantic salmon (Salmo salar) fed a diet containing perfluoroactane sulfonic or perfluorooctane carboxylic acids. Chemosphere 83 (8), 1035–1044. https://doi.org/10.1016/J.CHEMOSPHERE.2011.01.067.

Norwegian Environment Agency, 2020. Fem europeiske land vil ha generelt forbud mot PFASer - Miljødirektoratet. Retrieved May 18, 2020, from https://www.miljodirektoratet.no/aktuelt/nyheter/2020/mai-2020/fem-europeiske-land-vil-ha-generelt-forbud-mot-pfaser/.

Ojo, A.F., Peng, C., Ng, J.C., 2020. Combined effects and toxicological interactions of perfluoroalkyl and polyfluoroalkyl substances mixtures in human liver cells (HepG2). Environ. Pollut. 263, 114182. https://doi.org/10.1016/J.ENVPOL.2020.114182.

Ojo, A.F., Peng, C., Ng, J.C., 2021. Assessing the human health risks of per- and polyfluoroalkyl substances: a need for greater focus on their interactions as mixtures. J. Hazard. Mater. 407, 124863. https://doi.org/10.1016/J.JHAZMAT.2020.124863.

Olivares-Rubio, H.F., Vega-López, A., 2016. Fatty acid metabolism in fish species as a biomarker for environmental monitoring. Environ. Pollut. 218, 297–312. https://doi.org/10.1016/J.ENVPOL.2016.07.005.

Pfohl, M., Ingram, L., Marques, E., Auclair, A., Barlock, B., Jamwal, R., Anderson, D., Cummings, B.S., Slitt, A.L., 2020. Perfluorooctanesulfonic acid and perfluorohexanesulfonic acid alter the blood lipidome and the hepatic proteome in a murine model of diet-induced obesity. Toxicol. Sci. 178 (2), 311–324. https://doi.org/10.1093/toxsci/kfaa148.

Popovic, M., Zaja, R., Fent, K., Smital, T., 2014. Interaction of environmental contaminants with zebrafish organic anion transporting polypeptide, Oatp1d1 (Slco1d1). Toxicol. Appl. Pharmacol. 280 (1), 149–158. https://doi.org/10.1016/j.taap.2014.07.015.

Post, S.M., Groenendijk, M., Van Der Hoogt, C.C., Fievet, C., Luc, G., Hoekstra, M., Princen, H.M.G., Staels, B., Rensen, P.C.N., 2006. Cholesterol 7α-hydroxylase deficiency in mice on an APOE*3-Leiden background increases hepatic ABCA1 mRNA expression and HDL-cholesterol. Arterioscler. Thromb. Vasc. Biol. 26 (12), 2724–2730. https://doi.org/10.1161/01.ATV.0000247260.42560.e1.

Rashid, F., Ramakrishnan, A., Fields, C., Irudayaraj, J., 2020. Acute PFOA exposure promotes epigenomic alterations in mouse kidney tissues. Toxicol. Rep. 7, 125–132. https://doi.org/10.1016/J.TOXREP.2019.12.010.

Ren, H., Vallanat, B., Nelson, D.M., Yeung, L.W.Y., Guruge, K.S., Lam, P.K.S., Lehman-McKeeman, L.D., Corton, J.C., 2009. Evidence for the involvement of xenobiotic-responsive nuclear receptors in transcriptional effects upon perfluoroalkyl acid exposure in diverse species. Reprod. Toxicol. 27 (3–4), 266–277. https://doi.org/10.1016/J.REPROTOX.2008.12.011.

Rodea-Palomares, I., Makowski, M., Gonzalo, S., González-Pleiter, M., Leganés, F., Fernández-Piñas, F., 2015. Effect of PFOA/PFOS pre-exposure on the toxicity of the herbicides 2,4-D, atrazine, diuron and paraquat to a model aquatic photosynthetic microorganism. Chemosphere 139, 65–72. https://doi.org/10.1016/J.CHEMOSPHERE.2015.05.078.

Rousseau, M.E., Sant, K.E., Borden, L.R., Franks, D.G., Hahn, M.E., Timme-Laragy, A.R., 2015. Regulation of Ahr signaling by Nrf2 during development: effects of Nrf2a deficiency on PCB126 embryotoxicity in zebrafish (Danio rerio). Aquat.Toxicol. 167, 157–171. https://doi.org/10.1016/j.aquatox.2015.08.002.

Salkind, N., 2010. t test, paired sample. Encyclopedia of Research Design. SAGE Publications, Inc., 2455 Teller Road, Thousand Oaks California 91320 United States https://doi.org/10.4135/9781412961288.n477.

Sant, K.E., Sinno, P.P., Jacobs, H.M., Timme-Laragy, A.R., 2018. Nrf2a modulates the embryonic antioxidant response to perfluorooctanesulfonic acid (PFOS) in the zebrafish, Danio rerio. Aquat. Toxicol. 198, 92–102. https://doi.org/10.1016/J.AQUATOX.2018.02.010.

Sant, K.E., Annunziato, K., Conlin, S., Teicher, G., Chen, P., Venezia, O., Downes, G.B., Park, Y., Timme-Laragy, A.R., 2021. Developmental exposures to perfluorooctanesulfonic acid (PFOS) impact embryonic nutrition, pancreatic morphology, and adiposity in the zebrafish,Danio rerio. Environ. Pollut. 275, 116644. https://doi.org/10.1016/J.ENVPOL.2021.116644.

Söderström, S., Lille-Langøy, R., Yadetie, F., Rauch, M., Milinski, A., Dejaegere, A., Stote, R.H., Goksøyr, A., Karlsen, O.A., 2022. Agonistic and potentiating effects of perfluoroalkyl substances (PFAS) on the Atlantic cod (Gadus morhua) peroxisome proliferator-activated receptors (Ppars) Manuscript in review.

Søfteland, L., Holen, E., Olsvik, P.A., 2010. Toxicological application of primary hepatocyte cell cultures of Atlantic cod (Gadus morhua) — effects of BNF, PCDD and Cd. Comp. Biochem.Physiol.C Toxicol.Pharmacol. 151 (4), 401–411. https://doi.org/10.1016/J.CBPC.2010.01.003.

Star, B., Nederbragt, A.J., Jentoft, S., Grimholt, U., Malmstrøm, M., Gregers, T.F., Jakobsen, K.S., 2011. The genome sequence of Atlantic cod reveals a unique immune system. Nature 477 (7363), 207–210. https://doi.org/10.1038/nature10342.

Sturm, R., Ahrens, L., 2010. Trends of polyfluoroalkyl compounds in marine biota and in humans. Environ. Chem. 7 (6), 457–484. https://doi.org/10.1071/EN10072.

Subramanian, A., Tamayo, P., Mootha, V.K., Mukherjee, S., Ebert, B.L., Gillette, M.A., Paulovich, A., Pomeroy, S.L., Golub, T.R., Lander, E.S., Mesirov, J.P., 2005. Gene set enrichment analysis: a knowledge-based approach for interpreting genome-wide expression profiles. Proc. Natl. Acad. Sci. U. S. A. 102 (43), 15545–15550. https://doi.org/10.1073/pnas.0506580102.

Sundt, R.C., Ruus, A., Jonsson, H., Skarphéðinsdóttir, H., Meier, S., Grung, M., Beyer, J., Pampanin, D.M., 2012. Biomarker responses in Atlantic cod (Gadus morhua) exposed to produced water from a North Sea oil field: laboratory and field assessments. Mar. Pollut. Bull. 64 (1), 144–152. https://doi.org/10.1016/j.marpolbul.2011.10.005.

Tang, J., Jia, X., Gao, N., Wu, Y., Liu, Z., Lu, X., Du, Q., He, J., Li, N., Chen, B., Jiang, J., Liu, W., Ding, Y., Zhu, W., Zhang, H., 2018. Role of the Nrf2-ARE pathway in perfluorooctanoic acid (PFOA)-induced hepatotoxicity in Rana nigromaculata. Environ. Pollut. 238, 1035–1043. https://doi.org/10.1016/J.ENVPOL.2018.02.037.

Tarangelo, A., Dixon, S.J., 2019. Lipid metabolism and ferroptosis. Ferroptosis in Health And Disease. Springer International Publishing, Cham, pp. 1–26 https://doi.org/10.1007/978-3-030-26780-3_1.

Tikka, A., Jauhiainen, M., 2016. The role of ANGPTL3 in controlling lipoprotein metabolism. Endocrine 52, 187–193. https://doi.org/10.1007/s12020-015-0838-9.

Timme-Laragy, A.R., Karchner, S.I., Franks, D.G., Jenny, M.J., Harbeitner, R.C., Goldstone, J.V., McArthur, A.G., Hahn, M.E., 2012. Nrf2b, novel zebrafish paralog of oxidant-responsive transcription factor NF-E2-related factor 2 (NRF2). J. Biol. Chem. 287 (7), 4609–4627. https://doi.org/10.1074/jbc.M111.260125.

Tørresen, O.K., Star, B., Jentoft, S., Reinar, W.B., Grove, H., Miller, J.R., Walenz, B.P., Knight, J., Ekholm, J.M., Peluso, P., Edvardsen, R.B., Tooming-Klunderud, A., Skage, M., Lien, S., Jakobsen, K.S., Nederbragt, A.J., 2017. An improved genome assembly uncovers prolific tandem repeats in Atlantic cod. BMC Genomics 18 (1), 1–23. https://doi.org/10.1186/s12864-016-3448-x.

Wei, Y., Chan, L.L., Wang, D., Zhang, H., Wang, J., Dai, J., 2008. Proteomic analysis of hepatic protein profiles in rare minnow (Gobiocypris rarus) exposed to perfluorooctanoic acid. J. Proteome Res. 7 (4), 1729–1739. https://doi.org/10.1021/pr7008059.

Wei, Y., Shi, X., Zhang, H., Wang, J., Zhou, B., Dai, J., 2009. Combined effects of polyfluorinated and perfluorinated compounds on primary cultured hepatocytes from rare minnow (Gobiocypris rarus) using toxicogenomic analysis. Aquat. Toxicol. 95, 27–36. https://doi.org/10.1016/j.aquatox.2009.07.020.

Windom, H.L., 1992. Contamination of the marine environment from land-based sources. Mar. Pollut. Bull. 25 (1–4), 32–36. https://doi.org/10.1016/0025-326X(92)90180-E.

Wolf, C.J., Rider, C.V., Lau, C., Abbott, B.D., 2014. Evaluating the additivity of perfluoroalkyl acids in binary combinations on peroxisome proliferator-activated receptor-α activation. Toxicology 316, 43–54. https://doi.org/10.1016/J.TOX.2013.12.002.

Yadetie, F., Zhang, X., Hanna, E.M., Aranguren-Abadía, L., Eide, M., Blaser, N., Brun, M., Jonassen, I., Goksøyr, A., Karlsen, O.A., 2018. RNA-seq analysis of transcriptome responses in Atlantic cod (Gadus morhua) precision-cut liver slices exposed to benzo[a]pyrene and 17A-ethynylestradiol. Aquat. Toxicol. 201, 174–186. https://doi.org/10.1016/j.aquatox.2018.06.003.

Yadetie, F., Brun, N.R., Vieweg, I., Nahrgang, J., Karlsen, O.A., Goksøyr, A., 2021. Transcriptome responses in polar cod (Boreogadus saida) liver slice culture exposed to benzo[a]pyrene and ethynylestradiol: insights into anti-estrogenic effects. Toxicol. in Vitro 75, 105193. https://doi.org/10.1016/J.TIV.2021.105193.

Yang, C.H., Glover, K.P., Han, X., 2010. Characterization of cellular uptake of perfluorooctanoate via organic anion-transporting polypeptide 1A2, organic anion transporter 4, and urate transporter 1 for their potential roles in mediating human renal reabsorption of perfluorocarboxylates. Toxicol. Sci. 117 (2), 294–302. https://doi.org/10.1093/toxsci/kfq219.

Yang, H.-B., Zhao, Y.-Z., Tang, Y., Gong, H.-Q., Guo, F., Sun, W.-H., Liu, S.-S., Tan, H., Chen, F., 2019. Antioxidant defence system is responsible for the toxicological interactions of mixtures: a case study on PFOS and PFOA in Daphnia magna. Sci. Total Environ. 667, 435–443. https://doi.org/10.1016/J.SCITOTENV.2019.02.418.

Zhang, X., Jonassen, I., 2020. RASflow: an RNA-seq analysis workflow with snakemake. BMC Bioinformatics 21 (1), 110. https://doi.org/10.1186/s12859-020-3433-x.

Zhao, W., Zitzow, J.D., Weaver, Y., Ehresman, D.J., Chang, S.C., Butenhoff, J.L., Hagenbuch, B., 2017. Organic anion transporting polypeptides contribute to the disposition of perfluoroalkyl acids in humans and rats. Toxicol. Sci. 156 (1), 84–95. https://doi.org/10.1093/toxsci/kfw236.

Zheng, X.-M., Liu, H.-L., Shi, W., Wei, S., Giesy, J.P., Yu, H.-X., 2012. Effects of perfluorinated compounds on development of zebrafish embryos. Environ. Sci. Pollut. Res. 19 (7), 2498–2505. https://doi.org/10.1007/s11356-012-0977-y.